European Radiology (2019) 29:2408–2416
https://doi.org/10.1007/s00330-018-5893-1

HEPATOBILIARY-PANCREAS

How to utilize LR-M features of the LI-RADS to improve the diagnosis of combined hepatocellular-cholangiocarcinoma on gadoxetate-enhanced MRI?

Hong Seon Lee[1] · Myeong-Jin Kim[1] · Chansik An[1]

Received: 20 August 2018 / Revised: 23 October 2018 / Accepted: 14 November 2018 / Published online: 14 December 2018

Abstract

Objectives To investigate the diagnostic accuracy of each LR-M feature defined in version 2017 of the Liver Imaging Reporting and Data System (LI-RADS) and determine the optimal LR-M feature for differentiating combined hepatocellular-cholangiocarcinoma (cHCC-CCA) and hepatocellular carcinoma (HCC) on gadoxetate-enhanced magnetic resonance imaging (MRI).

Methods Ninety-nine patients with pathologically proven cHCC-CCA ($n = 33$) or HCC ($n = 66$) after surgery were identified. Two radiologists retrospectively assessed preoperative gadoxetate-enhanced MRI for features favoring non-HCC malignancies (LR-M features) according to LI-RADS version 2017. Multivariate logistic regression analysis was performed to determine the independent differential features. The sensitivity and specificity for diagnosing cHCC-CCA were calculated for each LR-M feature.

Results Targetoid appearance showed the highest sensitivity (75.8%, 95% confidence interval [CI] 60.6%, 87.3%) to correctly identify cHCC-CCA as LR-M. At least one LR-M feature was observed in 31 (93.9%) patients with cHCC-CCA and 34 (51.5%) patients with HCC. The sensitivity and specificity for diagnosing cHCC-CCA using the presence of any one of the LR-M features were 93.9% (95% CI 80.7, 98.9) and 48.5% (95% CI 41.9, 51.0), respectively. The presence of three LR-M features yielded the highest diagnostic accuracy of 80.8% (95% CI 72.1, 86.1) with a reduced sensitivity of 54.5% (95% CI 41.4, 62.5).

Conclusion The majority of cHCC-CCA cases can be properly categorized as LR-M when any one of the LR-M features defined in the LI-RADS version 2017 is used as a determiner. However, approximately half of HCC cases also show at least one LR-M feature.

Key Points

- *Targetoid appearance, including rim APHE, peripheral "washout" appearance, and delayed central enhancement, was the LR-M feature that identified cHCC-CCA as a non-HCC malignancy with the highest sensitivity.*
- *Most cHCC-CCA cases can be properly categorized as LR-M when the presence of any one of the LR-M features was used as the determiner.*
- *Approximately half of HCC cases also showed at least one LR-M feature.*

Keywords Liver neoplasm · Hepatocellular carcinoma · Magnetic resonance imaging · Gadolinium ethoxybenzyl DTPA · Contrast media

Abbreviations

APHE	Arterial phase hyperenhancement
cHCC-CCA	Combined hepatocellular-cholangiocarcinoma
DW	Diffusion-weighted
HBP	Hepatobiliary phase
HCC	Hepatocellular carcinoma
LI-RADS	Liver Imaging Reporting and Data System
v2017	version 2017
LR-M	Tumors with imaging features of malignancy that are not specific for HCC
MRI	Magnetic resonance imaging
TE	Echo time
TR	Repetition time

✉ Myeong-Jin Kim
KIMNEX@yuhs.ac

[1] Department of Radiology, Research Institute of Radiological Science, Severance Hospital, Yonsei University College of Medicine, 50-1 Yonsei-ro, Seodaemun-gu, Seoul 03722, South Korea

Introduction

Combined hepatocellular-cholangiocarcinoma (cHCC-CCA) is an uncommon hepatic malignancy that is characterized by

both hepatocytic and cholangiocytic differentiation and has been increasingly recognized recently [1]. The tumor tends to show poorer prognosis than HCC after curative resection or liver transplantation [2–5]. As HCC treatment is most commonly determined after diagnostic imaging, it would be clinically beneficial to distinguish cHCC-CCA from HCC at imaging diagnosis to establish the most suitable treatment [6, 7]. However, diagnostic performance for differentiating cHCC-CCA from HCC has been unsatisfactory [8–16].

According to the 2017 version of Liver Imaging Reporting and Data System (LI-RADS v2017) [17], tumors with imaging features of malignancy that are not specific for HCC are categorized as LR-M. Therefore, if cHCC-CCA can be categorized as LR-M on imaging, it can be correctly diagnosed by biopsy before definitive treatment. LR-M criteria are divided by either targetoid or nontargetoid mass with certain features. Targetoid appearance was defined as a tumor with at least one of the following imaging features: rim arterial phase hyperenhancement (APHE), delayed central enhancement, progressive concentric enhancement, peripheral washout, or target signs on diffusion-weighted (DW) or hepatobiliary phase (HBP) images [17]. Nontargetoid appearance includes infiltrative appearance, marked diffusion restriction, necrosis, severe ischemia, or other ancillary feature of various malignancies [18]. Recently, Potretzke et al [19] reported that most cHCC-CCA cases present imaging features indicating LR-M, based on analysis of CT or MRI of cHCC-CCA. In contrast, a controlled comparative study by Jeon et al [20] using gadoxetate-enhanced MRI showed that about 37% of cHCC-CCAs were categorized as LR-4 or LR-5, rather than LR-M. Therefore, how LR-M features should be utilized to improve diagnostic accuracy is still controversial. Moreover, it remains unknown how many cHCC-CCA or HCC cases show any of the LR-M features and which of the LR-M features yields the best diagnostic performance alone or in combination with other features. Therefore, the purposes of this study were to investigate the diagnostic accuracy of each LR-M feature defined in the LI-RADS v2017 and to determine the optimal LR-M features for differentiating cHCC-CCA and HCC on gadoxetate-enhanced magnetic resonance imaging (MRI).

Materials and methods

Patient selection

This retrospective study was approved by our Institutional Review Board, and the need for informed consent was waived. In total, 72 consecutive patients underwent liver MRI examination with pathologically confirmed cHCC-CCA between September 2008 and August 2016 at a single tertiary hospital. Of these, 26 patients were excluded because the preoperative MRI had been performed more than 2 months before surgery or without using gadoxetic acid. Thirteen additional patients were excluded due to the administration of loco-regional treatments or other anti-tumor therapies prior to the preoperative MRI. After these exclusions, 33 pathologically confirmed cHCC-CCA patients remained in the study. Among the 1157 patients who underwent preoperative MRI with surgically confirmed HCC, 66 patients were randomly selected for the control group within the same period by propensity matching for tumor size, MRI system, and underlying liver disease. Two of the 33 patients with cHCC-CCA had two or more lesions, but only one tumor from each patient was confirmed pathologically. Seven of the 66 patients with HCC had two or more pathologically proven HCCs. We decided to select the largest tumor from each patient to match the size of cHCC-CCA cases because only lesion was histologically confirmed in each patient of cHCC-CCA. Thus, a total of 33 patients with 33 cHCC-CCAs (26 men, 7 women; mean age, 58.6 years) and 66 patients with 66 HCCs (58 men, 8 women; mean age, 55.9 years) were included in the final analysis (Fig. 1 and Table 1).

MRI acquisition

MRI was performed using one of three 3.0-T systems (MAGNETOM Trio a Tim, Siemens Medical Solutions; Intera Achieva or Ingenia, Philips Medical Systems) or a 1.5-T system (Intera Achieva, Philips Medical Systems). Dual-echo T1-weighted gradient-recalled echo images were obtained after localization with the following parameters: section thickness/interval, 4–5 mm/2–2.5 mm; repetition time (TR), 4.0 ms/4.9 ms; and echo time (TE), 4.6 ms/2.3 ms (in-phase/opposed-phase) for the 1.5-T system and 2.3 ms/1.1–1.2 ms (in-phase/opposed-phase) for the 3.0-T systems.

A three-dimensional gradient-echo sequence was performed with chemically selective fat suppression before and after intravenous contrast agent injection (section thickness/interval, 4–5 mm/2–2.5 mm; TR/TE, 2.5–4.5 ms/0.9–1.7 ms). For dynamic imaging, gadoxetate disodium (0.025 mmol/kg; Primovist, Bayer Schering Pharma) was administered using a power injector at 1 mL/s as a rapid bolus followed by a saline flush of 20 mL. To obtain the optimal time window for arterial phase imaging, either a test bolus technique with 1 mL of gadoxetic acid or a bolus-tracking technique was used in all examinations. Following the arterial phase, portal venous phase and transitional phase images were obtained. HBP images were obtained 15–20 min after contrast injection. Portal venous phase images were considered to determine the presence of washout appearance, but transitional phase images were not.

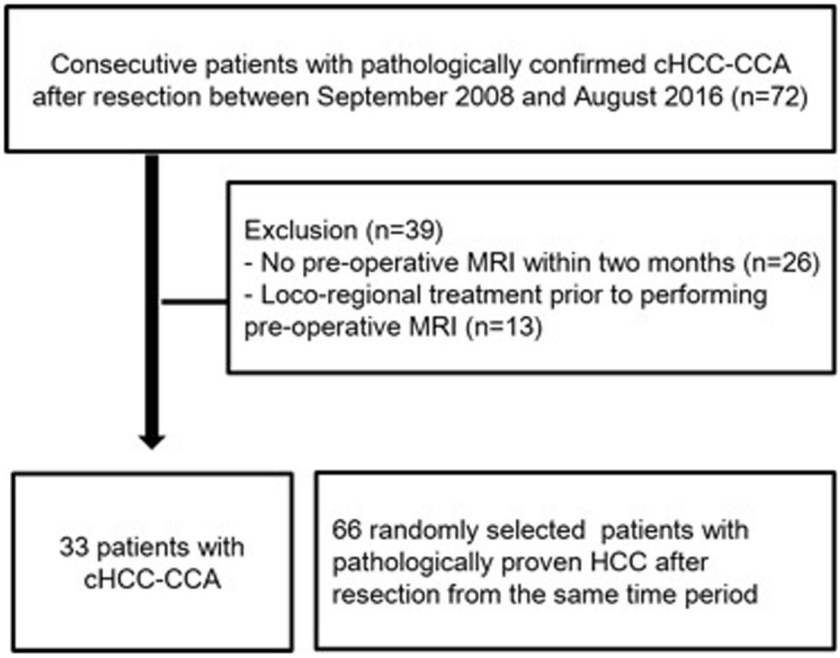

Fig. 1 Flowchart detailing the patient selection process and inclusion/exclusion criteria. In total, 33 patients with cHCC-CCA and 66 patients with HCC were included in the final analysis. cHCC-CCA, combined hepatocellular-cholangiocarcinoma; MRI, magnetic resonance imaging; HCC, hepatocellular carcinoma

During the interval between the transitional phase and HBP, T2-weighted images were acquired using multi-shot and single-shot turbo spin echo sequences with navigator triggering (slice thickness/interval, 4–5 mm/5–6 mm; TR/TE, 746–6531 ms/80–81 ms). DW images were also acquired with navigator triggering (section thickness/interval, 4–5 mm/5–6 mm; TR/TE, 4500–8500 ms/57–67 ms) at *b*-values of 50, 400, and 800 s/mm^2. The apparent diffusion coefficients were automatically calculated, and the corresponding apparent diffusion coefficient maps were displayed. Typical field-of-view was 40 cm but varied according to the patient's body size.

Image interpretation

One resident radiologist reviewed the pathologic data to be used as reference standards and summarized the patients' electronic medical records. Two radiologists with 24 and 6 years of experience (M.J.K. and C.A.) in abdominal imaging independently reviewed the MRI images. Both radiologists were blinded to the patients' clinical characteristics and pathologic diagnoses. They were aware that the examinations were selected from patients with cHCC-CCA and HCC, but they were not

Table 1 Clinico-pathologic characteristics of cHCC-CCA and HCC

Clinico-pathologic features	cHCC-CCA ($n = 33$)	HCC ($n = 66$)	p value
Age (years), mean ± SD	58.6 ± 12.8	55.9 ± 11.4	0.341
Sex (male:female)	26:7	58:8	0.248
Tumor size (cm), mean ± SD	4.2 ± 2.5	4.2 ± 2.2	0.379
Tumor marker			
AFP (ng/mL, range)	588.6 (2–13,013)	2496.6 (1–69,496)	0.062
PIVKA-II (mAU/mL, range)	520.3 (11–4096)	617.1 (10–8826)	0.853
Etiology			0.199
Hepatitis B virus (%)	19 (57.6%)	52 (78.8%)	
Hepatitis C virus (%)	3 (9.1%)	3 (4.5%)	
Alcoholic liver disease (%)	3 (9.1%)	5 (7.6%)	
None or unknown (%)	8 (24.2%)	6 (9.1%)	
Underlying liver disease			0.131
Liver cirrhosis (%)	17 (51.5%)	32 (48.5%)	
Chronic hepatitis (%)	11 (33.3%)	31 (47.0%)	
No liver disease (%)	5 (15.2%)	3 (4.5%)	

AFP α-fetoprotein, *cHCC-CCA* combined hepatocellular-cholangiocarcinoma, *HCC* hepatocellular carcinoma, *SD* standard deviation, *PIVKA-II* protein induced by vitamin K absence II

informed about the exact ratio of the two groups. The presence or absence of each LR-M feature as defined in the LI-RADS version 2017 was recorded. The LR-M features included rim APHE, delayed central enhancement, progressive concentric enhancement, peripheral washout, target sign on DW or HBP images, liver surface retraction, adjacent biliary obstruction, mixed pattern, and infiltrative margin. Targetoid appearance was defined as a tumor with at least one of following imaging features: rim APHE, delayed central enhancement, progressive concentric enhancement, peripheral washout, or target signs on DW or HBP images (Figs. 2, 3, and 4) [17]. Disagreements between the two reviewers were resolved in a second review, and a consensus opinion was achieved.

Statistical analysis

Differences in age and tumor size were evaluated with independent *t* tests, and differences in tumor marker levels were evaluated with Mann-Whitney *U* tests. Chi-squared or Fisher's exact tests were performed to compare the sex ratio, etiology of liver disease, liver disease status, and frequency of each imaging feature. Inter-observer agreement was assessed for the presence of each imaging feature using κ statistics with the ranges 0.81–1.0, 0.61–0.80, 0.41–0.60, 0.21–0.40, and 0.00–0.20 corresponding to almost perfect, substantial, moderate, fair, and slight, respectively. The accuracy, sensitivity, and specificity of the each LR-M feature for differentiating between cHCC-CCA and HCC were calculated based on the consensus data with 95% confidence intervals (CIs). Multivariate logistic regression analysis was performed to investigate the predictive value of each imaging feature for diagnosis of cHCC-CCA. Variables with a p value < 0.2 from the univariate analysis were subjected to multivariate analysis. For multivariate analyses, rim APHE, delayed central enhancement, progressive concentric enhancement, peripheral washout, and target signs on DW or HBP images were grouped into targetoid appearance. Statistical significance was set at $p < 0.05$. All statistical analyses were performed using SPSS version 23.0 (IBM).

Results

The clinical and tumor characteristics of patients in the cHCC-CCA and HCC groups are summarized in Table 1. No significant differences in age, sex, tumor size, tumor markers, or the proportion of underlying liver disease were noted between the two groups ($p > 0.05$). Inter-observer agreement for the presence of each LR-M feature was mostly substantial to almost perfect (Table 2). Among all the LR-M features, six features, including rim APHE, progressive concentric enhancement, peripheral washout, adjacent biliary obstruction, mixed pattern, and infiltrative margin, were significantly more common in patients with cHCC-CCA than in patients with HCC ($p < 0.05$). Further, these LR-M features exhibited sensitivities of 21.2–57.6% and specificities of 78.8–97.0% for the

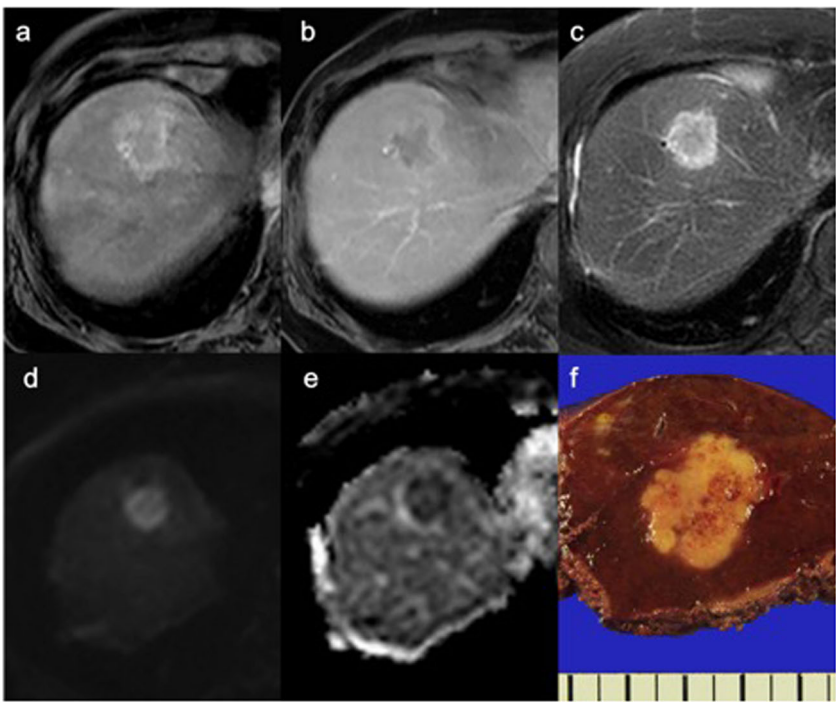

Fig. 2 A combined hepatocellular-cholangiocarcinoma in a 67-year-old man with B-viral cirrhosis showing LR-M features. **a** Gadoxetate-enhanced arterial and **b** portal venous phase images show a mass with irregular margins, rim-like arterial phase hyperenhancement, and washout appearance. **c** T2-weighted fast-spin echo, **d** diffusion-weighted ($b = 800$ s/mm^2), and **e** apparent diffusion coefficient map images show the mass with targetoid pattern. **f** The surgical specimen shows the mass with an irregular infiltrative margin

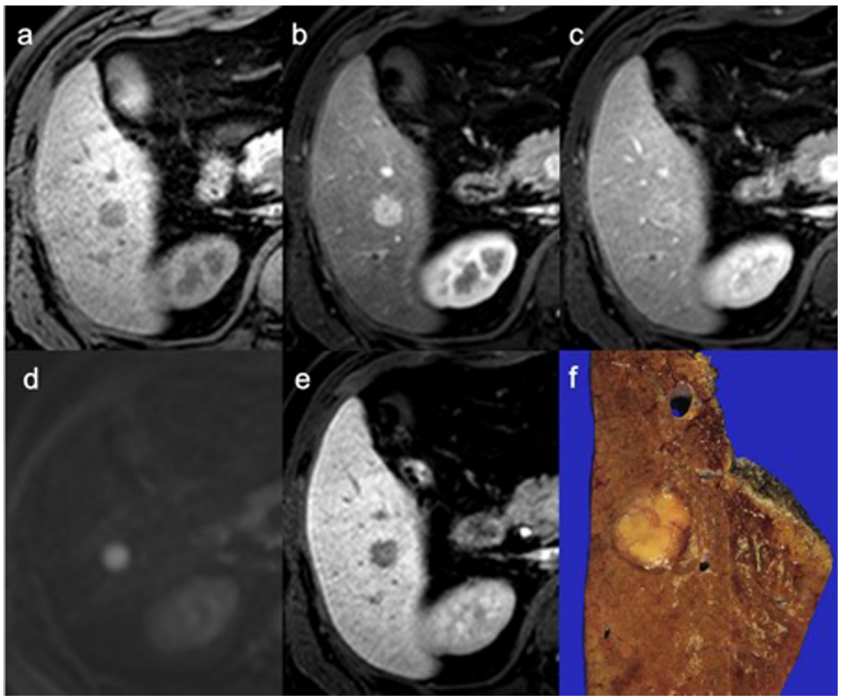

Fig. 3 A combined hepatocellular-cholangiocarcinoma mimicking HCC in a 51-year-old man with B-viral hepatitis. **a** Precontrast, **b** gadoxetate-enhanced arterial, and (**c**) portal venous phase images show a homogenously hypervascular nodule with both capsule and washout appearance. **d** The diffusion-weighted image ($b = 800$ s/mm^2) shows a homogeneously hyperintense mass without a targetoid pattern. **e** The hepatobiliary phase image shows a hypointense mass with hypointense rim. **f** The surgical specimen shows a mass with partial encapsulation

diagnosis of cHCC-CCA (Table 3). Representative examples of patients with cHCC-CCA with LR-M features, cHCC-CCA mimicking HCC, and HCC with LR-M features are shown in Figs. 2, 3, and 4, respectively. Targetoid appearance, a composite finding of five LR-M features, was significantly more common in the cHCC-CCA group with a diagnostic sensitivity of 75.8% (95% CI 60.6%, 87.3%) and a specificity of 65.2% (95% CI 57.6%, 70.9%). Among the findings that are included in the targetoid appearance, rim APHE (57.6% [95% CI 43.1%, 69.5%]) was the most sensitive individual LR-M finding.

When the presence of at least one LR-M feature was used to diagnose cHCC-CCA, the sensitivity was 93.9% (95% CI 80.7%, 98.9%) with a specificity of 48.5% (95% CI 41.9%, 51.0%). The use of three or more LR-M features yielded the highest accuracy but reduced sensitivity for identifying cHCC-CCA. Univariate logistic regression analysis of targetoid appearance, adjacent biliary obstruction, mixed pattern, and infiltrative margin showed significant association with cHCC-CCA (Table 4). The results of multivariate analysis showed that targetoid appearance, adjacent biliary obstruction, and infiltrative margin were selected as independent features.

Discussion

According to the current LI-RADS, LR-M category indicates an observation probably or definitely malignant but not specific for HCC [18]. LR-M criteria are defined by two types of imaging patterns: targetoid and nontargetoid. Targetoid appearance includes targetoid enhancement (rim APHE, peripheral "washout" appearance, or delayed central enhancement), targetoid restriction on DW images, or targetoid enhancement on transitional or HBP images. Nontargetoid mass with infiltrative appearance, marked diffusion restriction, necrosis or severe ischemia, or other feature that suggestive of non-HCC also can be categorized as LR-M.

Our study showed that the collective imaging features grouped into targetoid appearance were the most sensitive LR-M features that identifying cHCC-CCA as a non-HCC malignancy. Of these features, the rim APHE was the single most sensitive feature included in targetoid appearance. We also found that the majority of cHCC-CCA cases could be optimally categorized as LR-M with a high sensitivity (93.9%) and modest specificity (48.5%) if the presence of any one of the LR-M features defined in the LI-RADS version 2017 was used for the differentiation of cHCC-CCA from HCC. Our results are contrary to a recent report by Jeon et al [20], where 37.1% of cHCC-CCAs were categorized either LR-4 or LR-5. However, in their study, the categorization of LR-M/4/5 was not strictly based on the presence of certain LR-M features. Alternatively, our findings are comparable with the results of Potretzke et al [19] who found that 93.4% of cHCC-CCAs showed at least one ancillary feature favoring non-HCC malignancy. In our study, we further evaluated the incidence of each LR-M feature in patients with HCC and found that 51.5% of HCCs also present at least one LR-M feature.

Importantly, in the present study, the overall accuracy for the differentiation of cHCC-CCA was the highest when the presence of three or more LR-M features was used as the determiner. However, the use of this criterion may substantially

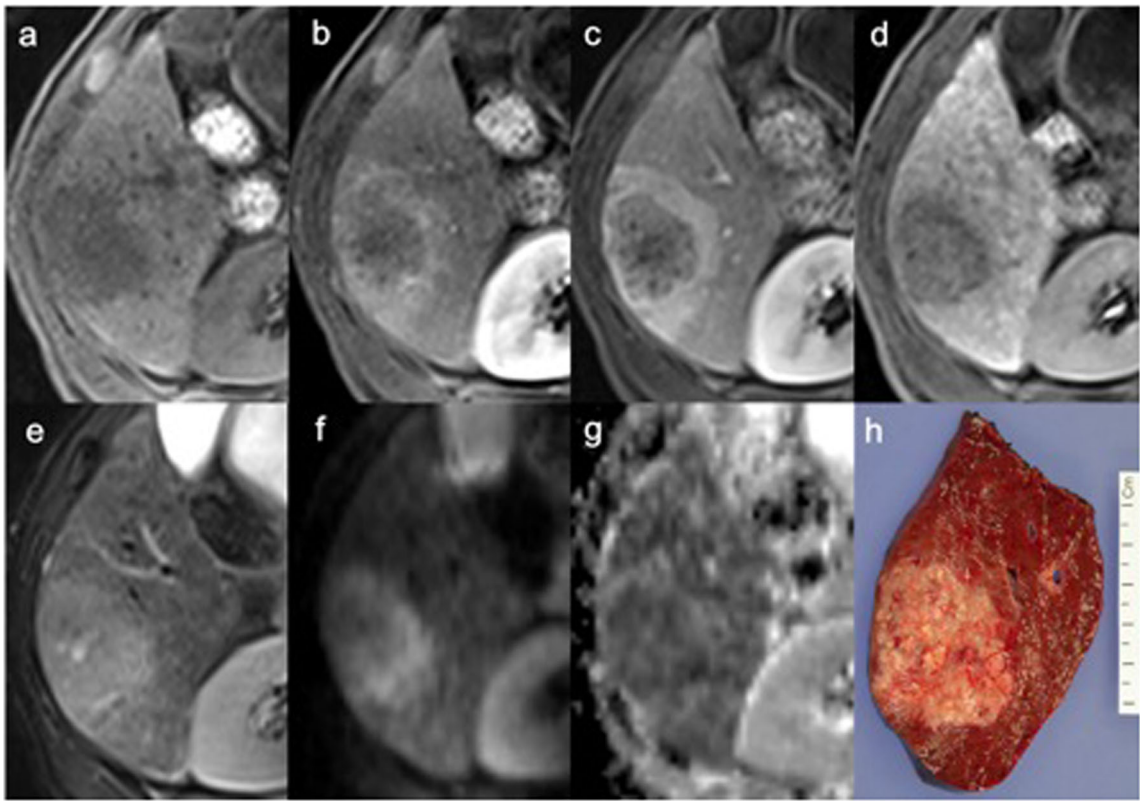

Fig. 4 A hepatocellular carcinoma in a 50-year-old man with B-viral cirrhosis showing LR-M features. **a** The precontrast T1-weighted gradient-echo in-phase image shows a hypointense mass with an irregular margin. **b** Gadoxetate-enhanced arterial and (**c**) portal venous phase images show a rim-like enhancing mass with progressive enhancement. **d** The hepatobiliary phase image shows delayed central enhancement. The mass also shows a targetoid pattern on (**e**) T2-weighted, (**f**) diffusion-weighted ($b = 800$ s/mm^2), and (**g**) apparent diffusion coefficient map images. **h** The gross specimen shows a mass with an infiltrative margin

decrease the sensitivity for the identification of cHCC-CCA. Heightened sensitivity for categorizing cHCC-CCA as LR-M is most vital when the accurate identification of patients with non-HCC malignancies is important, such as in determining candidates for liver transplantation. On the other hand, the relatively low specificity of LR-M features for diagnosing cHCC-CCA in our results implies that a larger proportion of LR-M lesions will eventually be diagnosed as HCC. In a study based on prospective application of the LI-RADS categorization, Kim et al [21] reported that 76.9% of LR-M cases were eventually diagnosed as HCC. Further, according to our experience, LR-M features are more common in surgically ineligible cases. Therefore, as the present study included only patients who had undergone surgical resection, the incidence of HCC exhibiting LR-M features may have been artificially lowered. Moreover, considering that the incidence of HCC is almost 20 times higher than that of cHCC-CCA, the clinical burden and potential complications related to the procedure could substantially increase if all tumors showing any LR-M feature are categorized as LR-M and undergo biopsy. According to the very recently revised version of the LI-RADS (v2018), LR-M can be reported with different descriptions based on each LR-M feature and imaging features suggesting hepatocellular origin [22]. The utility of this approach should be further investigated in future studies. Nonetheless, considering that patients with HCC presenting with LR-M features may have a worse prognosis [23], discriminating whether HCCs are LR-4,

Table 2 Inter-observer agreement of LR-M features

LR-M features	κ value
Rim APHE	0.866
Delayed central enhancement	0.649
Progressive concentric enhancement	0.647
Peripheral washout	0.580
Target sign on DW or HBP images	0.503
Liver surface retraction	0.565
Adjacent biliary obstruction	0.703
Mixed pattern	0.681
Infiltrative margin	0.794

APHE arterial phase hyperenhancement, *DW* diffusion-weighted, *HBP* hepatobiliary phase

κ values 0.81–1.0, 0.61–0.80, 0.41–0.60, 0.21–0.40, and 0.00–0.20 correspond to almost perfect, substantial, moderate, fair, and slight, respectively

Table 3 Comparison of the presence of LR-M features between cHCC-CCA and HCC

LR-M features	cHCC-CCA ($n = 33$)	HCC ($n = 66$)	Accuracy (%)*	Sensitivity (%)*	Specificity (%)*	p value
Targetoid appearance†	25 (75.8%)	23 (34.8%)	68.7 (58.6, 76.4)	75.8 (60.6, 87.3)	65.2 (57.6, 70.9)	< 0.001
Rim APHE	19 (57.6%)	10 (15.2%)	75.8 (66.1, 83.7)	57.6 (43.1, 69.5)	84.8 (77.6, 90.8)	< 0.001
Delayed central enhancement	5 (15.2%)	6 (9.1%)	65.7 (59.7, 72.1)	15.2 (6.3, 24.8)	90.9 (86.5, 95.7)	0.499
Progressive concentric enhancement	12 (36.4%)	2 (3.0%)	76.8 (69.1, 80.1)	36.4 (24.8, 41.3)	97.0 (91.2, 99.5)	< 0.001
Peripheral washout	9 (27.3%)	4 (6.1%)	71.7 (64.2, 77.0)	27.3 (14.0, 35.2)	93.9 (88.3, 97.9)	0.009
Target sign on DW or HBP images	7 (21.2%)	10 (15.2%)	63.6 (56.5, 71.7)	21.2 (10.5, 33.2)	84.8 (79.5, 90.9)	0.573
Liver surface retraction	3 (9.1%)	1 (1.5%)	68.7 (64.4, 70.6)	9.1 (2.7, 12.0)	98.5 (95.3, 99.9)	0.107
Adjacent biliary obstruction	7 (21.1%)	3 (4.5%)	70.7 (64.0, 75.1)	21.2 (11.1, 27.8)	95.5 (90.4, 98.7)	0.015
Mixed pattern	7 (21.2%)	4 (6.1%)	69.7 (52.9, 74.9)	21.2 (11.0, 29.1)	93.9 (88.8, 97.9)	0.039
Infiltrative margin	17 (51.5%)	14 (21.2%)	69.7 (59.9, 78.6)	51.5 (36.9, 64.8)	78.8 (71.5, 85.4)	0.003
Number of each LR-M feature						
At least 1 LR-M feature	31 (93.9%)	34 (51.5%)	63.6 (54.8, 67.0)	93.9 (80.7, 98.9)	48.5 (41.9, 51.0)	0.000
2 or more LR-M features	24 (72.7%)	14 (21.2%)	76.8 (66.9, 84.5)	72.7 (57.9, 84.3)	78.8 (71.4, 84.6)	0.000
3 or more LR-M features	18 (54.5%)	4 (6.1%)	80.8 (72.1, 86.1)	54.5 (41.4, 62.5)	93.9 (87.4, 97.9)	0.000
4 or more LR-M features	9 (27.3%)	2 (3.0%)	73.7 (66.6, 77.1)	27.3 (16.6, 32.2)	97.0 (91.6, 99.5)	0.001

cHCC-CCA combined hepatocellular-cholangiocarcinoma, *HCC* hepatocellular carcinoma, *APHE* arterial phase hyperenhancement, *DW* diffusionweighted, *HBP* hepatobiliary phase, *PPV* positive predictive value, *NPV* negative predictive value

*Data in parentheses are 95% confidence intervals of percentage

† Targetoid appearance: at least one of following imaging features: rim APHE, delayed central enhancement, progressive concentric enhancement, peripheral washout, and target signs on DW or HBP images

LR-5, or LR-M has important clinical implications related to the patient's prognosis.

In the present study, three LR-M features, namely targetoid appearance, infiltrative margin, and adjacent biliary obstruction, were selected for multivariate analysis for the differentiation of cHCC-CCA and HCC. However, the use of only those independent features did not appear to improve diagnostic accuracy. Our study also showed that among the LR-M features, the presence of a targetoid appearance yielded the highest sensitivity (75.8%) for diagnosing cHCC-CCA. This is not surprising given that targetoid appearance is a collective feature including both targetoid enhancement (rim APHE, peripheral washout, or delayed central enhancement) and targetoid appearance (targetoid transitional phase or HBP signal intensity or targetoid restriction) according to the LI-RADS v2017. Among these features, rim APHE alone showed a sensitivity of 57.6% and a specificity of 84.9% for diagnosing cHCC-CCA in the present study. This result supports the discrimination of rim-like APHE from global APHE, as is done in the LI-RADS v2017 [24, 25]. Our results imply that the presence of targetoid appearance could be used as a strong indicator of non-HCC malignancies including cHCC-CCA. In contrast, three LR-M features, namely liver surface retraction, delayed central enhancement, and target signs on DW or HBP images, were not statistically significant for differentiating cHCC-CCA from HCC in our series. Although these findings were previously reported to be useful for differentiating cholangiocarcinomas [26–28], they were relatively uncommon in our series in patients with cHCC-CCA which may more frequently show findings similar to HCC [19, 29]. Compared to studies by Fraum et al [8] which used either CT or MRI (either gadoxetate or extracellular contrast material)

Table 4 Univariate and multivariate analyses of LR-M features

	Univariate		Multivariate	
	Odds ratio	p value	Odds ratio	p value
Targetoid appearance	5.842 (2.274, 15.009)	0.000	4.113 (1.429, 11.840)	0.009
Liver surface retraction	6.500 (0.649, 65.102)	0.111	10.755 (0.858, 134.780)	0.066
Adjacent biliary obstruction	5.654 (1.356, 23.569)	0.017	5.284 (1.011, 27.606)	0.048
Mixed pattern	4.173 (1.125, 15.482)	0.033	3.510 (0.743, 16.578)	0.113
Infiltrative margin	3.946 (1.601, 9.730)	0.003	4.227 (1.480, 12.076)	0.007

Data in parentheses are 95% confidence intervals

and by Jeon et al [19] that used gadoxetate-enhanced MRI, delayed enhancement was more commonly visible in cHCC-CCA than in our study, but less commonly seen in HCC than in ours. These results suggest that the nonsignificant difference of delayed central enhancement in our study cannot be attributed to the use of gadoxetate as a contrast material, but may be due to differences of study population or differences in reviewers' identification of the presence of imaging findings.

Our study also showed that rim APHE provided the highest kappa value with excellent inter-observer agreement, as well as the most common individual finding in cHCC-CCA, followed by infiltrative margin and progressive concentric enhancement, which also showed substantial agreement. On the other hand, findings such as peripheral washout, target signs on DW or HBP images, and liver surface retraction showed only moderate agreement. The modest agreement of some of the LR-M features was also noted in previous results [8, 30], suggesting the necessity of further clarification for the definition of those imaging findings as well as further assessment of their significance in a larger consecutive series. In the present study, we did not evaluate the utility of some LR-M features mentioned in the LI-RADS v2017, including marked diffusion restriction, necrosis, or severe ischemia, because the imaging definitions of these features have not been clearly documented, and, thus, we deemed they would incur higher inter-observer variability.

Our study also showed that a small proportion of cHCC-CCAs may not be categorized as LR-M. Specifically, two of the 33 (6%) cHCC-CCAs were not deemed to show any LR-M features. This result is consistent with that of the study by Potretzke et al [19]. According to our experience, the lack of LR-M features in cHCC-CCA may be more common in small (< 2 cm) tumors. However, as the pathologist's awareness of cHCC-CCA is increasing [1], the incidence of tumors showing both non-rim APHE and washout appearance without prominent LR-M features may also increase.

Our study has several limitations. First, we did not include the entirety of the consecutive HCC cases for the analysis, because the number of HCC cases was much larger than that of cHCC-CCA. Therefore, we randomly sampled twice the number of HCC cases among all diagnosed HCCs during the same period when the cHCC-CCAs were diagnosed. We used this method to avoid any condition where the reviewers might have been biased by the higher prevalence of HCC. However, we also acknowledge that the artificially higher proportion of cHCC-CCA in our study subjects might have introduced higher rate of appreciation of LR-M features. A future prospective study in a series of consecutive patients may be warranted. To our knowledge, there has been only one controlled comparative study regarding the differentiation of cHCC-CCA and HCC [20] where the same number of HCCs and cHCC-CCAs was compared. We increased the number of HCCs to reflect the larger prevalence of HCC. Second, as we only included surgically proven cHCC-CCAs and HCCs, selection bias could have been induced. However, as our results have shown, cHCC-CCAs have the potential to be misinterpreted as HCCs based on imaging alone. Combined with the fact that exact diagnosis is sometimes difficult by biopsy, the inclusion of only surgically proven cases is warranted. Third, as cHCC-CCA is relatively rare tumor, the cases were collected over a long period of time and examined with different MRI systems. Therefore, image quality was not the same in all patients. However, as we matched the time frame of MRI examination between groups of HCC and cHCC-CCA, the MRI techniques and protocols were comparable between the two groups. Actually, there had been only minor modifications of imaging protocols during the time period and the imaging protocol was comparable in all patients. Fourth, we conducted our study using LI-RADS v2017. We noted that LI-RADS v2018 has been introduced online very recently. However, the definition of LR-M and its imaging features has not been changed. Fifth, we did not include cases of cholangiocarcinomas or metastases that can also frequently be categorized as LR-M, as our intention was to evaluate the diagnostic performance of the current LR-M criteria for the differentiation of cHCC-CCA, which we considered the most difficult diagnostic entity to be differentiated from HCC in cirrhotic liver. A larger cohort study including various forms of non-HCC malignancy would be warranted to define the overall diagnostic performance of LR-M criteria. Finally, since this was a retrospective, single-center study, our results should be validated in a larger, multi-center study.

In conclusion, our study showed that targetoid appearance was the most sensitive imaging finding to identify cHCC-CCA as a non-HCC malignancy and most cHCC-CCA cases can be properly categorized as LR-M with high sensitivity and modest specificity when the presence of any one of the LR-M features defined in the LI-RADS version 2017 was used as the determiner for the differentiation from HCC.

Funding The authors state that this work has not received any funding.

Compliance with ethical standards

Guarantor The scientific guarantor of this publication is Myeong-Jin Kim.

Conflict of interest The authors of this manuscript declare no relationships with any companies, whose products or services may be related to the subject matter of the article.

Statistics and biometry No complex statistical methods were necessary for this paper.

Informed consent Written informed consent was waived by the Institutional Review Board.

Ethical approval Institutional Review Board approval was obtained.

Methodology
- retrospective
- case-control study
- performed at one institution

References

1. Brunt E, Aishima S, Clavien PA et al (2018) cHCC-CCA: consensus terminology for primary liver carcinomas with both hepatocytic and cholangiocytic differentation. Hepatology 68:113–126
2. Yoon YI, Hwang S, Lee YJ et al (2016) Postresection outcomes of combined hepatocellular carcinoma-cholangiocarcinoma, hepatocellular carcinoma and intrahepatic cholangiocarcinoma. J Gastrointest Surg 20:411–420
3. Yin X, Zhang BH, Qiu SJ et al (2012) Combined hepatocellular carcinoma and cholangiocarcinoma: clinical features, treatment modalities, and prognosis. Ann Surg Oncol 19:2869–2876
4. Magistri P, Tarantino G, Serra V, Guidetti C, Ballarin R, Di Benedetto F (2017) Liver transplantation and combined hepatocellular-cholangiocarcinoma: feasibility and outcomes. Dig Liver Dis 49:467–470
5. Vilchez V, Shah MB, Daily MF et al (2016) Long-term outcome of patients undergoing liver transplantation for mixed hepatocellular carcinoma and cholangiocarcinoma: an analysis of the UNOS database. HPB (Oxford) 18:29–34
6. European Association for the Study of the Liver (2018) EASL clinical practice guidelines: management of hepatocellular carcinoma. J Hepatol 69:182–236
7. Heimbach JK, Kulik LM, Finn RS et al (2018) AASLD guidelines for the treatment of hepatocellular carcinoma. Hepatology 67:358–380
8. Fowler KJ, Sheybani A, Parker RA 3rd et al (2013) Combined hepatocellular and cholangiocarcinoma (biphenotypic) tumors: imaging features and diagnostic accuracy of contrast-enhanced CT and MRI. AJR Am J Roentgenol 201:332–339
9. Fraum TJ, Tsai R, Rohe E et al (2018) Differentiation of hepatocellular carcinoma from other hepatic malignancies in patients at risk: diagnostic performance of the Liver Imaging Reporting and Data System version 2014. Radiology 286:158–172
10. Mao Y, Xu S, Hu W et al (2017) Imaging features predict prognosis of patients with combined hepatocellular-cholangiocarcinoma. Clin Radiol 72:129–135
11. Park SH, Lee SS, Yu E et al (2017) Combined hepatocellular-cholangiocarcinoma: gadoxetic acid-enhanced MRI findings correlated with pathologic features and prognosis. J Magn Reson Imaging 46:267–280
12. Sheng RF, Xie YH, Ji Y et al (2016) MR comparative study of combined hepatocellular-cholangiocarcinoma in normal, fibrotic, and cirrhotic livers. Abdom Radiol (NY) 41:2102–2114
13. Maximin S, Ganeshan DM, Shanbhogue AK et al (2014) Current update on combined hepatocellular-cholangiocarcinoma. Eur J Radiol Open 1:40–48
14. Shetty AS, Fowler KJ, Brunt EM, Agarwal S, Narra VR, Menias CO (2014) Combined hepatocellular-cholangiocarcinoma: what the radiologist needs to know about biphenotypic liver carcinoma. Abdom Imaging 39:310–322
15. de Campos RO, Semelka RC, Azevedo RM et al (2012) Combined hepatocellular carcinoma-cholangiocarcinoma: report of MR appearance in eleven patients. J Magn Reson Imaging 36:1139–1147
16. Hwang J, Kim YK, Park MJ et al (2012) Differentiating combined hepatocellular and cholangiocarcinoma from mass-forming intrahepatic cholangiocarcinoma using gadoxetic acid-enhanced MRI. J Magn Reson Imaging 36:881–889
17. Elsayes KM, Hooker JC, Agrons MM et al (2017) 2017 version of LI-RADS for CT and MR imaging: an update. Radiographics 37:1994–2017
18. Fowler KJ, Potretzke TA, Hope TA, Costa EA, Wilson SR (2018) LI-RADS M (LR-M): definite or probable malignancy, not specific for hepatocellular carcinoma. Abdom Radiol (NY) 43:149–157
19. Potretzke TA, Tan BR, Doyle MB, Brunt EM, Heiken JP, Fowler KJ (2016) Imaging features of biphenotypic primary liver carcinoma (hepatocholangiocarcinoma) and the potential to mimic hepatocellular carcinoma: LI-RADS analysis of CT and MRI features in 61 cases. AJR Am J Roentgenol 207:25–31
20. Jeon SK, Joo I, Lee DH et al (2018) Combined hepatocellular cholangiocarcinoma: LI-RADS v2017 categorisation for differential diagnosis and prognostication on gadoxetic acid-enhanced MR imaging. Eur Radiol. https://doi.org/10.1007/s00330-018-5605-x
21. Kim YY, An C, Kim S, Kim MJ (2018) Diagnostic accuracy of prospective application of the Liver Imaging Reporting and Data System (LI-RADS) in gadoxetate-enhanced MRI. Eur Radiol 28:2038–2046
22. (2018) CT/MRI LI-RADS® v2018. Available via https://www.acr.org/Clinical-Resources/Reporting-and-Data-Systems/LI-RADS/CT-MRI-LIRADSv2018. Accessed 8 Aug 2018
23. An C, Park S, Chung YE et al (2017) Curative resection of single primary hepatic malignancy: liver imaging reporting and data system category LR-M portends a worse prognosis. AJR Am J Roentgenol 209:576–583
24. Tang A, Bashir MR, Corwin MT et al (2018) Evidence supporting LI-RADS major features for CT- and MR imaging-based diagnosis of hepatocellular carcinoma: a systematic review. Radiology 286:29–48
25. Park HJ, Jang KM, Kang TW et al (2016) Identification of imaging predictors discriminating different primary liver tumours in patients with chronic liver disease on gadoxetic acid-enhanced MRI: a classification tree analysis. Eur Radiol 26:3102–3111
26. Park MJ, Kim YK, Park HJ, Hwang J, Lee WJ (2013) Scirrhous hepatocellular carcinoma on gadoxetic acid-enhanced magnetic resonance imaging and diffusion-weighted imaging: emphasis on the differentiation of intrahepatic cholangiocarcinoma. J Comput Assist Tomogr 37:872–881
27. Park HJ, Kim YK, Park MJ, Lee WJ (2013) Small intrahepatic mass-forming cholangiocarcinoma: target sign on diffusion-weighted imaging for differentiation from hepatocellular carcinoma. Abdom Imaging 38:793–801
28. Kang Y, Lee JM, Kim SH, Han JK, Choi BI (2012) Intrahepatic mass-forming cholangiocarcinoma: enhancement patterns on gadoxetic acid-enhanced MR images. Radiology 264:751–760
29. Li R, Yang D, Tang CL et al (2016) Combined hepatocellular carcinoma and cholangiocarcinoma (biphenotypic) tumors: clinical characteristics, imaging features of contrast-enhanced ultrasound and computed tomography. BMC Cancer 16:158
30. Horvat N, Nikolovski I, Long N et al (2018) Imaging features of hepatocellular carcinoma compared to intrahepatic cholangiocarcinoma and combined tumor on MRI using liver imaging and data system (LI-RADS) version 2014. Abdom Radiol (NY) 43:169–178